applied sciences

MDPI

Article

Analysis of Steel Wire Rope Diagnostic Data Applying Multi-Criteria Methods

Audrius Čereška [1], Edmundas Kazimieras Zavadskas [2,*], Vytautas Bucinskas [3], Valentinas Podvezko [4] and Ernestas Sutinys [5]

1 Department of Mechanical and Material Engineering, Vilnius Gediminas Technical University, Basanaviciaus str. 28, Vilnius LT-03324, Lithuania; audrius.cereska@vgtu.lt
2 Institute of Sustainable Construction, Vilnius Gediminas Technical University, Sauletekio al. 11, Vilnius LT-10223, Lithuania
3 Department of Mechatronics, Robotics and Digital Manufacturing, Vilnius Gediminas Technical University, Basanaviciaus str. 28, Vilnius LT-03324, Lithuania; vytautas.bucinskas@vgtu.lt
4 Department of Mathematical Statistics, Vilnius Gediminas Technical University, Sauletekio al. 11, Vilnius LT-10223, Lithuania; valentinas.podvezko@vgtu.lt
5 Department of Mechatronics, Robotics and Digital Manufacturing, Vilnius Gediminas Technical University, Basanaviciaus str. 28, Vilnius LT-03324, Lithuania; ernestas.sutinys@vgtu.lt
* Correspondence: edmundas.zavadskas@vgtu.lt; Tel.: +370-698-20779

Received: 19 January 2018; Accepted: 5 February 2018; Published: 9 February 2018

Abstract: Steel ropes are complex flexible structures used in many technical applications, such as elevators, cable cars, and funicular cabs. Due to the specific design and critical safety requirements, diagnostics of ropes remains an important issue. Broken wire number in the steel ropes is limited by safety standards when they are used in the human lifting and carrying installations. There are some practical issues on loose wires—firstly, it shows end of lifetime of the entire rope, independently of wear, lubrication or wrong winding on the drums or through pulleys; and, secondly, it can stick in the tight pulley—support gaps and cause deterioration of rope structure up to birdcage formations. Normal rope operation should not generate broken wires, so increasing of their number shows a need for rope installation maintenance. This paper presents a methodology of steel rope diagnostics and the results of analysis using multi-criteria analysis methods. The experimental part of the research was performed using an original test bench to detect broken wires on the rope surface by its vibrations. Diagnostics was performed in the range of frequencies from 60 to 560 Hz with a pitch of 50 Hz. The obtained amplitudes of the broken rope wire vibrations, different from the entire rope surface vibration parameters, was the significant outcome. Later analysis of the obtained experimental results revealed the most significant values of the diagnostic parameters. The evaluation of the power of the diagnostics was implemented by using multi-criteria decision-making (MCDM) methods. Various decision-making methods are necessary due to unknown efficiencies with respect to the physical phenomena of the evaluated processes. The significance of the methods was evaluated using objective methods from the structure of the presented data. Some of these methods were proposed by authors of this paper. Implementation of MCDM in diagnostic data analysis and definition of the diagnostic parameters significance offers meaningful results.

Keywords: steel wire rope; rope diagnostics; dynamic methods; MCDM; objective criteria weight

1. Introduction

Steel ropes consisting of wound strands of wires have a long history of implementation in technical installations. Steel ropes are widely used starting from static support of buildings and bridges to moving force transmission in elevators and cable cars. Due to their thin structure and the fact that

ropes are the most loaded components in critical safety installations, such as passenger elevators, periodic quality control and maintenance is obligatory for installations with ropes [1–11].

Defects of the ropes develop from exploitation based effects: mechanical wear, cracks from bending fatigue, corrosion, overload, and shear cracks. Steel rope quality degeneration process is very gradual; it never breaks instantly, wires are broken sequentially and at random places.

There are plenty of methods for cable diagnostics. The oldest method of rope examination is optical inspection, which is still in use, but it remains expensive and inefficient with modern applications. There are more methods, such as acoustic field, electromagnetic [1,4,5,12,13] and X-ray, but they are hardly applicable for broken wire defects. The above mentioned diagnostic methods often fail at finding broken wires on steel rope surfaces. Dirty and oily ropes in real applications can be inspected much more efficiently using transversal vibrations of rope fragments, where the rope fragment ends are fixed. During the vibration process broken wires clean themselves and can be noticed by using vibration sensors.

The analysis of the rope defects and its diagnostics are impossible without a proper understanding of the rope mechanics and the development of realistic models. There are many analytical and numerical models; a primary role of the latter belongs to the method of finite element modeling (FEM). The proposed models of the rope evaluate different phenomena.

Giglio and Manes developed a model for seven rope strands with an independent core, evaluating stresses and fatigue, but omitting contact and friction influences [14]. There is research on twisted 6×36 IWRC and straight 18×7 IWRC structure of the rope, where stresses and torque are evaluated, but the contact influence was neglected with infinite friction [15]. An improved model of the 6×19 rope strand contacts and friction evaluated the mechanism of heat generation in the rope [16], but general behavior of the rope was left behind. Modern FEM model of two-layered rope fragments evaluated all possible contacts between wires, dry friction, small deflections and deformations, torque, and bending moments [17], thus explaining behavior of the rope structure using static loads. Further analysis of the rope dynamics is required to decrease amount of calculation, therefore a 3D linear FEM element for the definition of friction between wires and the rope core was developed [18,19]. Development of more comprehensive FEM models of one strand of the rope in the mode of elastic deformation really diminished differences between numerical calculations and experimental research. Using such analysis, promising results with strong correlation between them and experimental measurements were obtained [20]. Influence of variable strand pitch to other rope mechanical properties was successfully modeled and tested using factory-produced rope [21], thus proving optimal strand pitch value. Material properties as well as polymer use in the steel ropes with a polymer core influences rope exploitation process, and a proposed methodology of fault finding in the internal layer brings new perspectives to the field of rope diagnostics [22].

A significant amount of research has been performed in the field of practical defectoscopy, i.e. the research and development of rope defect detecting equipment. A well-known rope control device, which implemented magnetic field analysis, is presented in [23]. A magnetic field delivers comprehensive information about ferromagnetic media; this way various defects of the rope can be detected. However, multibody systems significantly distort magnetic fields and a single broken wire may remain undetected. Recently, a method and device appeared that utilizes the remaining magnetic field in ferromagnetic materials (RMF), and has advantages against other magnetic methods in accuracy and convenience due to the compact and light nature of the device. Practical implementation of RMF confirms its usefulness in defect-finding and small friction value between sensor tip with testing the rope surface [13,24,25].

The presented papers deliver extensive results into the research of rope diagnostics and fault finding. On the other hand, research on the rope quality dependence from amount of broken wires in the rope is still missing. The detection of broken wires on the rope surface is performed using optical inspection, therefore, implementation of new methods and devices is requested [2–5].

With data obtained from sensors after signal processing, there are rare cases when the signal offers a clear case of damage. The definition of damage with high possibility is given by the multi-criteria decision-making (MCDM) methods, which takes into account the general dataset from the hardware and derives a solution after objective data analysis. In MCDM methods, definition of criteria weights is an important stage. In the practical implementation of MCDM methods, criteria weights are defined be experts. In our case, subjective evaluation of the criteria weights is not applicable, because experts have difficulty in defining criteria weights. Therefore, it is possible to define criteria weights using objective criteria weight definition methods. These weights are used in the MCDM methods to define the best alternative or aligning alternatives according to importance. In technical diagnostics, the implementation of decision-making procedures has a great potential.

In many real cases, there exists a need to evaluate a situation described by more than one criteria, therefore MCDM methods are used. These methods become especially useful for research of sustainability and reliability, when few criteria of efficiency are evaluated at the same time.

Implementation of MCDM methods in the field of engineering can be illustrated by comprehensive research of steel structures, steel bridges (method of Analytical Hierarchy Process (AHP)) [26], and cold-formed Hun-walled steel structures [27]. Extensive implementation of The Technique for Order of Preference by Similarity to Ideal Solution (TOPSIS) methods in steel buildings [28] gained success and was extended to wider technological area. Welding processes are evaluated using MCDM with fuzzy logic [29], while laser cutting technological parameters are defined using AHP-TOPSIS [30]. There are many methods for thin-walled structure evaluation using Complex Proportional Assessment (COPRAS) [31–37], which confirms the implementation of these methods in the field of engineering.

The modified method of AHP-COPRAS-G was successfully used for cold-formed steel structure design [38], where the strict physical conditions of material creates high nonlinearities of the mathematical formulation. Non-uniform task for cutting tool material selection [39] and structural materials selection [40–43] also finely fit into the area of MCDM. Proper selection of machine tools for changing production flow has been performed using fuzzy AHP and COPRAS methods [44].

The aim of this paper is to perform diagnostics of wire rope by finding broken wires using dynamic methods and process the obtained results with multi-criteria analysis. Analysis of the broken wire amplitude from its length and applied vibration frequency remains an important issue. Data, obtained from extensive diagnostics process, require special processing, which will reveal the true defect with a possibly high chance. The evaluation of results will be processed using multi-criteria decision-making methods (MCDM): Evaluation based on Distance from Average Solution (EDAS) [45], Simple Additive Weighting (SAW) [46], TOPSIS [46], and COPRAS [47]. Here, the criteria weight is defined by objective methods, which evaluate the structure of the analyzed data. The widely-used method of entropy [48], which provides criteria value diversification, is not sensitive in the main tasks of diagnostics. New methods (Criterion Impact Loss (CILOS)) [49,50] and Integrated Determination of Objective Criteria Weights (IDOCRIW) [50], proposed by the authors, compensate the deficiencies of the entropy method.

2. Object of Research and the Test Rig

Experimental research was performed on various diameters (3.92, 3.96 and 4.0 mm) and lengths (1350, 1450 and 1550 mm) of 6 × 19 IWRC steel rope, as shown in Figure 1. The specimens were prepared so that various lengths of loose wires were sticking from the surface. During the experimental research, the broken wires should be detected by a vibration sensor and the vibration of wire should differ from the vibration of the rope surface.

The first result of this experimental research was the excitation of a broken wire by exciting the whole rope in cross-section, significantly remote from the broken wire. Excitement of the wire was observed in frequency ranges lower than the calculated ones with the oscillations having significant amplitude, noticed even by eye. Vibration displacements of the rope surface and tip of broken wire were measured with reliable Hottiger inductive contactless sensors, represented in Figure 2 as positions

9 (rope surface) and 11 (wire tip), correspondingly. Acquired sensor data are processed by original amplifier, presented on digital monitor, and transmitted via serial cable to computer COM port. Data from COM port via apps are delivered to Origin spreadsheet for further processing. The methodology of this experimental research was described in [5], and the method has been successfully patented.

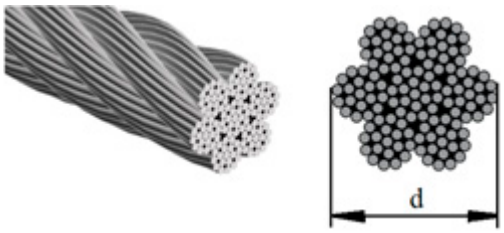

Figure 1. Steel rope 6 × 19 IWRC; d is the actual diameter of the rope.

For research of the rope and broken wire dynamic behavior, a special test rig was designed and produced, as presented in Figure 2 [1,5].

Figure 2. Test rig vibration measuring diagram: 1, frame; 2, rope support; 3, rope support; 4, test rope; 5, holder of transducer Tr4; 6, linear transducer "Hottiger Tr102"; 7, linear transducer "Hottiger Tr4"; 8, power amplifier 2706; 9, amplifier "Hottiger KWS 503 D"; 10, signal generator 1027; 11, electrodynamic mini vibrator 4810; 12, holder of transducer Tr102; and 13, broken wire.

3. Methodology of Wire Rope Research

The possibility to find a broken wire is based on the difference of natural frequencies between the rope and its broken wire. Due to wearing of the rope, its diameter can decrease about 5%, but a single wire takes less than 1% of the actual cross-section. Influence of single broken wire to overall stiffness

of entire rope is insignificant, therefore analysis of longitudinal and rotational rope stiffness brings poor results [6]. It is possible to find the presence and position of such defect increases in the case of vibration of free end of wire with different parameters as vibrations of entire rope surface [1].

The length of broken wire varies in the range from one winding of a strand to one-half of a winding. In addition, it is necessary to note that broken wires will float to the external rope surface due to bending and tension forces. The main parts of industrial ropes are single-wound or cross-wound; cross-linked types are not used in the mentioned technical installations.

To define defect on the rope surface using dynamic method, there is a need to create a model of such broken wire, considering the connection between rope and wire body. Successful implementation of theoretical model of Timoshenko beam for such structures brings prospective to use such model in the presented case [51,52]. Nevertheless, the boundary conditions in such model, as shown in Figure 3, are obtained from experimental results [5].

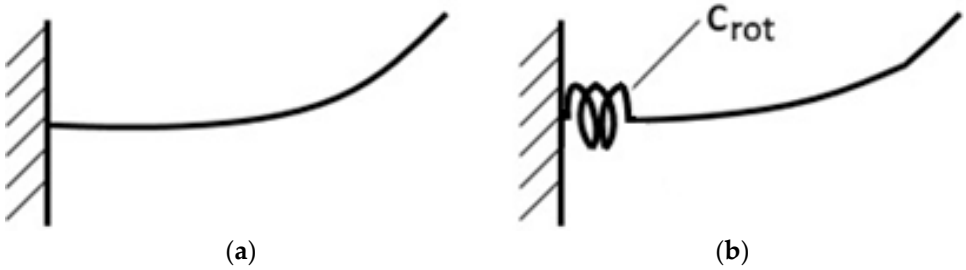

Figure 3. Type of Timoshenko beam connection to the ground: (**a**) fixed; and (**b**) through elastic spring with rotational stiffness C_{rot}.

Timoshenko beam model can be implemented, when few conditions are respected. First, beam stiffness should conform to the condition in Equation (1) [53], which defines limits of object dimensions and material properties for the beam:

$$\frac{EI}{\kappa L^2 AG} << 1, \tag{1}$$

where L is the length of the beam, A is the cross-section area of the beam, E is the elastic modulus of material, G is the shear modulus, I is the second moment of area, and κ is called the Timoshenko shear coefficient, which depends on the geometry. Normally, $\kappa = 9/10$ for a circular section. In the case of broken wire, this condition is obviously respected. If the condition is violated and beam is too long, elasticity of material cannot withstand its own gravitational force.

An important second condition defines frequency limit, as stated in Equation (2) [54]. In our case, critical frequency is far beyond the limit, especially when diagnostic method is focused in first natural frequency modes.

Such approximation of broken wire has critical angular frequency ω_c and is given as:

$$\omega_c = 2\pi f_c = \sqrt{\frac{\kappa GA}{\rho I}}, \tag{2}$$

where ρ is density of the material of the beam.

Implementation of Timoshenko beam model lets us define ranges of testing frequencies for the broken wire, where vibration amplitudes of the rope surface and broken wire are significantly different.

It is important to note that the entire rope body is treated as tensed wire with special properties [15], the behavior of which is different from Timoshenko beam, where shear properties of the rope remain unclear. Experimental research have proven the initial assumptions on frequency range; damping in this case plays little role.

Further obtained results of broken wire natural frequencies, as presented in the Table 1, fix the conditions to Case (a), as presented in Figure 3.

For the first set of ropes, the actual broken wire diameter is $d = 0.26$ mm $= 0.26 \times 10^{-3}$ m. The actual length of the broken wire is $l = 17.0$ mm $= 17.0 \cdot 10^{-3}$ m. The amplitudes of the vibrations as a dynamic response to the forced excitations depend on damping and, in this case, we leave it open, because our diagnostic method is based on the differences between the amplitudes of the rope and the loose wire. In advance, it is known [3,6] that the damping ratio in the rope may highly exceed the damping values on broken wires.

Experimental research was performed on well-tensed steel rope with broken wires of various lengths. All tests were performed in two stages:

1. Initially, the amplitudes of different lengths of broken wires on the rope surface were measured with harmonic excitation applied; the frequency range of the vibrations were from 60 Hz to 560 Hz.
2. Vibration amplitudes of the rope surface and broken wires were measured synchronously with the excitation of the rope at various frequencies.

Such a technique allows finding the sensitive frequency response areas, where wires vibrate with greater amplitude than the entire rope, which means significantly fewer experiments. Testing in a higher frequency range requires greater energy for exciting the rope and greater losses in friction between strands and wires.

The Steel Wire Rope Diagnostic Research Results

Experimental tests were performed after applying tension to the rope, corresponding to 90% of static nominal load. Vibration was applied from an electrodynamic mini-vibrator in the transverse direction to the rope axis. The exciting vibration amplitude is adjusted so that, during the shift of frequency, it remains permanent. Measurement of the vibration amplitudes of the rope and broken wires was taken simultaneously when the rope was excited on remote places from contactless sensors.

Rope diameters for the experimental research were taken from industrial needs: 3.92, 3.96 and 4.0 mm diameter ropes are widely used in elevators due to the small diameter and small bending radius. Small differences of broken wire vibrating amplitudes bring advantages for the method; diagnosed ropes of close diameter use the same settings. Diameters of the ropes outside diameter range should be set for different diagnostic frequencies.

Tension of the entire rope fragment will alter the natural frequency of the rope itself; the natural frequency changes of broken wires can be neglected. Broken wires are not influenced by tension, as they have free ends. Damping effects in the rope are very large, therefore, decaying of the rope vibrations are significant, but this does not affect the essence of the diagnostic method.

The implemented method measures only the relative vibration of a broken wire with respect to the surface of the rope. Here, it is important to obtain the relative vibrations; otherwise, only rope surface vibrations will be measured.

The obtained graphs of results for the 1350 mm rope are presented in Figure 4.

Practical implementation of this method is in the tension station of the elevator between two pulleys. Extra fixture for the rope is placed there and the test is performed as on a test rig. After the test, the next part of rope is tested, previously sliding to next fragment between the pulleys. Test in the field conditions: wire fragment rate is 1300 mm (for practical range of the overall tensed rope frequency when rope is from 3.8 to 6 mm); 1500 mm when length is from 6 to 12 mm. The minimal radius tested was limited by practical dimensions used in elevator, typically 4–6 mm.

From experimental results, it is evident that the broken wires are successfully excited, therefore, their amplitudes are significantly higher than the rope surface. Using various diameters and lengths of rope, in the range of frequencies from 115 Hz to 182 Hz, diagnostic features became efficient. Graphically efficient areas of vibration diagnostics are presented in Figure 4. Of course, various lengths

of broken wires have different natural frequencies, but they are in a technically convenient frequency range. Wires with 8–10 mm lengths have maximum amplitudes that occur at a frequency of 160 Hz. In the case the exciting frequency equals 160 Hz and the rope length and diameter are 1350 mm and 3.92 mm, respectively, a 10 mm broken wire generates an amplitude of 11.6 mm. All the data correspond to the case when broken wires have higher amplitude and there is a possibility to detect the existence of such a wire.

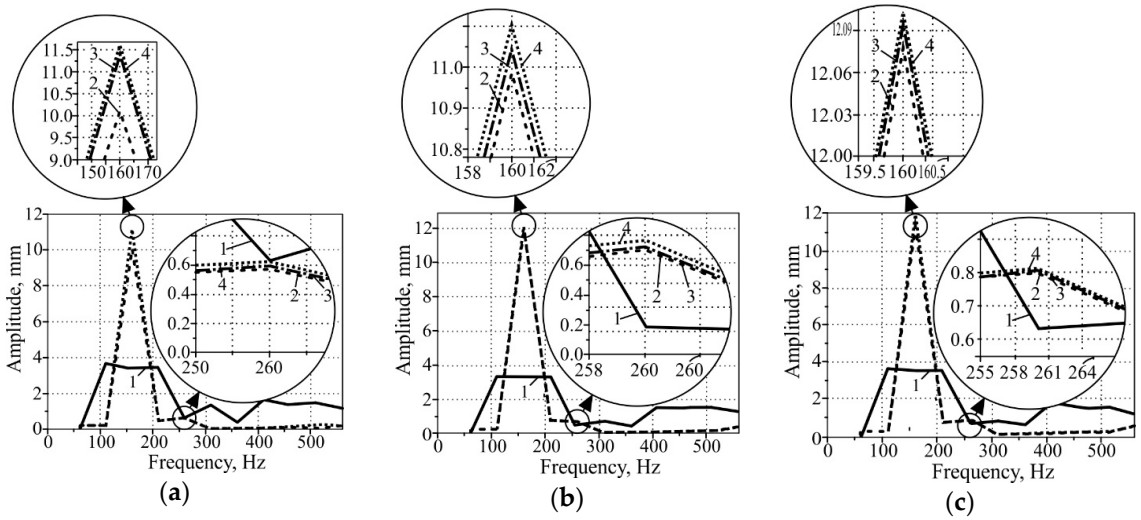

Figure 4. Amplitude–frequency characteristics of a 1350 mm length rope and broken wires: (**a**) actual diameter of the rope, 3.92 mm; (**b**) actual diameter of the rope, 3.96 mm; and (**c**) actual diameter of the rope, 4.0 mm (1, rope vibration amplitude; 2, 10 mm length broken wire; 3, 9 mm length broken wire; and 4, 8 mm length broken wire).

The experimental data presented in Table 1 show a sample of the overall data. All experimental data can be found in Appendix A (Table A1).

Table 1. Structure of rope vibration experimental data.

Item No.	Frequency, Hz	Rope Length, mm	Rope Diameter, mm	Rope Amplitude, mm	10 mm Wire Amplitude, mm	9 mm Wire Amplitude, mm	8 mm Wire Amplitude, mm
1	60	1350	3.92	0.082	0.237	0.223	0.233
2		1450		0.124	0.226	0.362	0.295
3		1550		0.119	0.364	0.385	0.402
4		1350	3.96	0.087	0.284	0.291	0.289
5		1450		0.110	0.228	0.279	0.299
6		1550		0.120	0.288	0.285	0.287
7		1350	4.0	0.056	0.199	0.231	0.212
8		1450		0.132	0.305	0.294	0.291
9		1550		0.121	0.299	0.288	0.301
1	110	1350	3.92	3.648	0.198	0.184	0.174
2		1450		3.502	0.202	0.226	0.235
3		1550		3.495	0.351	0.352	0.349
4		1350	3.96	3.523	0.214	0.199	0.174
5		1450		3.891	0.198	0.199	0.188
6		1550		3.315	0.258	0.281	0.252
7		1350	4.0	3.598	0.184	0.201	0.187
8		1450		3.871	0.279	0.284	0.289
9		1550		3.498	0.288	0.283	0.286

The experimental test proved the frequencies over 258 Hz had caused amplitudes of broken wire vibrations equal to the entire rope vibration amplitudes. Therefore, there is no need to continue raising the frequency for ropes of the tested diameter.

The most promising is the frequency range between 115 Hz and 182 Hz; as the variable dynamic response amplitude of the rope, the broken wires are sensitive to this frequency range.

4. Implemented MCDM Methods

The purpose of MCDM methods is to define which of compared alternatives (cases) A_1, A_2, ..., A_n is the best, or the order of alternatives in respect to importance of purpose. Evaluation process is characterized by criteria (indicators and factors) R_1, R_2, ..., R_m. The MCDM methods are based on the decision matrix $R = \|r_{ij}\|$ statistical data of criteria, values of technological parameters or expert evaluations, and vector of criteria importance (weights) $\Omega = (\omega_j)$, where $I = 1, 2, ..., n$; $j = 1, 2, ..., m$; m is number of criteria; and n is number of evaluated alternatives.

The main idea of MDCM methods is joining of evaluation criteria values and their weights to single evaluation characteristics—i.e., criteria of the method. MCDM methods implement the maximized (beneficial) criterion, in the case where maximum value of criteria corresponds the best one (profit, for example), and the minimized one, when the best value of criteria is minimal (expenses, for example).

Recently, many MCDM methods are available [55]. Every method has its own logics, advantages and deficiencies. This paper presents research that implemented the main ideas of MCDM methods. Obtained experimental results were analyzed using several MCDM methods: EDAS (Evaluation Based on Distance from Average Solution) [45], SAW (Simple Additive Weighting) [46], TOPSIS (The Technique for Order of Preference by Similarity to Ideal Solution) [46,47,56] and COPRAS (Complex Proportional Assessment) [47,57]. SAW combines the criteria values and weights to obtain a single point of reference for evaluation, i.e., the method's criterion. Nevertheless, SAW requires rearranging indicators from minimization to maximization values. COPRAS compensates this deficiency and separately evaluates influence of maximized and minimized indicators. TOPSIS defines alternatives by the distances between the best and worst values of indicators. EDAS evaluates distance of each alternative from the cases built using criteria mean values.

Weight of criteria were obtained using methods of entropy [48], criteria loss CILOS (Criterion Impact LOS) [49,50] and generalized IDOCRIW [50] (Integrated Determination of Objective Criteria Weights). These methods have been used to solve mechanic [58], environmental [59], and civil engineering [60,61] problems.

4.1. EDAS Method

The EDAS (Evaluation Based on Distance from Average Solution) [45,59–61] method is similar to the TOPSIS method. In the TOPSIS method, the desirable alternative has a lower distance from the ideal solution and a higher distance from the nadir solution. In the EDAS method, the best alternative is related to the distance from the average solution [45]. In this method, we have two measures dealing with the desirability of the alternatives. The first measure is the positive distance from the average (PD), and the second is the negative distance from the average (ND). The evaluation of the alternatives is made according to higher values of PD and lower values of ND. The steps for using the EDAS method are presented as follows:

Step 1: Construct the decisions matrix (R):

$$R = \|r_{ij}\|, \tag{3}$$

Create the criterion statistics (experimental criterion values) and criteria weights vector [46]:

$$\Omega = (\omega_j), \tag{4}$$

where $i = 1, 2, ..., n$; $j = 1, 2, ..., m$; m is the number of criteria; and n is the number of compared options [20].

Step 2: Calculate the average of all criteria:

$$AV_j = \sum_{i=1}^{n} r_{ij}/n, \tag{5}$$

Step 3: Calculate the positive distance from the average (PD) and the negative distance from the average (ND):

$$PD_{ij} = \frac{\max\left(0, \left(r_{ij} - AV_j\right)\right)}{AV_j}, \tag{6}$$

$$ND_{ij} = \frac{\max\left(0, \left(AV_j - r_{ij}\right)\right)}{AV_j}, \tag{7}$$

where the j-th criterion is maximized (beneficial), and:

$$PD_{ij} = \frac{\max\left(0, \left(AV_j - r_{ij}\right)\right)}{AV_j}, \tag{8}$$

$$ND_{ij} = \frac{\max\left(0, \left(r_{ij} - AV_j\right)\right)}{AV_j}, \tag{9}$$

where the j-th criterion is minimized (non-beneficial), and PD_{ij} and ND_{ij} denote the positive and negative distance of the i-th alternative from the average solution in terms of j-th criterion, respectively.

Step 4: Determine the weighted sum of PD and ND for all alternatives:

$$SP_i = \sum_{j=1}^{m} w_j PD_{ij}, \tag{10}$$

$$SN_i = \sum_{j=1}^{m} w_j ND_{ij}, \tag{11}$$

where ω_j is the weight of j-th criterion.

Step 5: Normalize the values of SP and SN for all alternatives:

$$NSP_i = \frac{SP_i}{\max_i SP_i}, \tag{12}$$

$$NSN_i = 1 - \frac{SN_i}{\max_i SN_i}, \tag{13}$$

Step 6: Calculate the appraisal score (AS) for all alternatives:

$$AS_i = \frac{1}{2}(NSP_i + NSN_i), \tag{14}$$

where $0 \leq AS_i \leq 1$.

4.2. SAW Method

The basic idea behind MCDM methods is to combine the criteria values and weights to obtain a single point of reference for evaluation, i.e., the method's criterion. A common example is SAW [46], where the evaluation criterion of the method S_i is calculated the following (15):

$$S_i = \sum_{j=1}^{m} w_j \widetilde{r}_{ij}, \tag{15}$$

where w_j is the weight of the j-th criterion and $\widetilde{r}_{ij}$ is the normalized (dimensionless) value of the j-th criterion for the i-th alternative:

$$\widetilde{r}_{ij} = \frac{r_{ij}}{\sum_{i=1}^{n} r_{ij}}. \tag{16}$$

4.3. TOPSIS Method

The method TOPSIS [46,56] is based on vector normalization:

$$\widetilde{r}_{ij} = \frac{r_{ij}}{\sqrt{\sum_{i=1}^{n} r_{ij}^2}} \quad (i = 1, \ldots, n;\ j = 1, \ldots, m), \tag{17}$$

where $\widetilde{r}_{ij}$ is the normalized value of j-th criterion for i-th alternative.

The best alternative V^* and the worst alternative V^- are calculated by:

$$V* = \{V_1^*, V_2^*, \ldots, V_m^*\} = \{(\max_i \omega_j \widetilde{r}_{ij} \ / \ j \in J_1), (\min_i \omega_j \widetilde{r}_{ij} / \ j \in J_2)\}, \tag{18}$$

$$V^- = \{V_1^-, V_2^-, \ldots, V_m^-\} = \{(\min_i \omega_j \widetilde{r}_{ij} / \ j \in J_1), (\max_i \omega_j \widetilde{r}_{ij} / \ j \in J_2)\}, \tag{19}$$

where J_1 is a set of indices of the maximized criteria, and J_2 is a set of indices of the minimized criteria.

The distance D_i^* of every considered alternative to the ideal (best) solutions and its distance D_i^- to the worst solutions are calculated:

$$D_i^* = \sqrt{\sum_{j=1}^{m} (\omega_j \widetilde{r}_{ij} - V_j^*)^2}, \tag{20}$$

$$D_i^- = \sqrt{\sum_{j=1}^{m} (\omega_j \widetilde{r}_{ij} - V_j^-)^2}, \tag{21}$$

The criterion C_i^* of the method TOPSIS is calculated by:

$$C_i^* = \frac{D_i^-}{D_i^* + D_i^-} (i = 1, \ldots, n), (0 \le C_i^* \le 1). \tag{22}$$

The largest value of the criterion C_i^* corresponds to the best alternative.

4.4. COPRAS Method

The criterion of the method COPRAS [47,57], Z_i, is calculated:

$$Z_i = S_{+i} + \frac{\sum_{i=1}^{n} S_{-i}}{S_{-i} \sum_{i=1}^{n} \frac{1}{S_{-i}}}, \tag{23}$$

where $S_{+i} = \sum_{j=1}^{m} \omega_j \widetilde{r}_{+ij}$ is the sum of the weighted values of the maximized criteria $\widetilde{r}_{+ij}$, and $S_{-i} = \sum_{j=1}^{m} \omega_j \widetilde{r}_{-ij}$ is the same for the minimized criteria.

To calculate the values of the criterion Z_i, a method for the normalization of the initial data based on Equation (16) is applied.

4.5. Methods of Criteria Weight Definition

Recently, in practice subjective criteria weights are used, provided by experts. In this particular case, experts cannot evaluate influence of applied factors to the results of research. During moment of evaluation, it is impossible to consider the structure of the data and define real degree of criteria domination, i.e., their objective weights. In recent practice, objective methods are rare in comparison

to subjective ones. Therefore, there are such methods as entropy, the Criterion Impact Loss (CILOS) and the Integrated Determination of Objective Criteria Weights (IDOCRIW).

The widely used method of entropy evaluates dependency of criteria weights from their dominating degree, i.e., the extent of data diversification is considered. Proposed by the authors, CILOS defines relative loss of criteria in the case when other criteria are assumed to be optimal. In this case, small criteria loss is assigned a great weight, and vice versa—big loss of criteria causes insignificant weight. Proposed by the authors of this paper, IDOCRIW joins weights of both methods to common weights of objective structure array. In this way, deficiencies of one method are compensated by the advantages of other methods.

4.5.1. Entropy Method

The entropy method [62] was offered by Claude E. Shannon [48]. Entropy weights (in normalized form) are defined as follows [46,50]:

1. The values of criteria are normalized using Equation (24):

$$\widetilde{r}_{ij} = \frac{r_{ij}}{\sum_{i=1}^{n} r_{ij}}, \tag{24}$$

2. The entropy level of each criterion is calculated as follows:

$$E_j = -\frac{1}{\ln n}\sum_{i=1}^{n} \widetilde{r}_{ij} \cdot \ln \widetilde{r}_{ij}, \left(j = 1, 2, \ldots, m; \quad 0 \le E_j \le 1\right), \tag{25}$$

3. The variation level of each criterion is calculated:

$$d_j = 1 - E_j, \tag{26}$$

4. Entropy weights are calculated using normalized values d_j:

$$W_j = \frac{d_j}{\sum_{j=1}^{m} d_j}, \tag{27}$$

Entropy weights reflect the structure of the data, the degree of its non-homogeneity. The weight of homogeneous data (when the values of the criteria do not differ considerably) obtained by the entropy method [50] is about zero and does not have a strong influence on evaluation. The largest weight of the criterion obtained by using the entropy method corresponds to the criterion with the highest weight ratio.

4.5.2. Method of Criterion Impact Loss (CILOS)

This is another promising method of criteria impact loss and determination of objective weights [49]. The method evaluates the loss of each criterion, until one of the remaining criteria acquires the optimum—the maximum or the minimum value. The algorithm of the method, formalization, description, and application have been presented [50]. The logic of the method of criteria significance loss, the basic ideas, stages and the calculation algorithm are given below.

The minimized criteria have been transformed to maximizing according to the following equation:

$$\bar{r}_{ij} = \frac{\min_i r_{ij}}{r_{ij}}, \tag{28}$$

The new matrix is denoted as $X = \|x_{ij}\|$. The maximum values of each column, i.e., every criterion, are calculated: $x_j = max_i\, x_{ij} = x_{kjj}$, where k_{jj} is the number of the row of jth column, and the largest value is attained.

A square matrix $A = \|a_{ij}\|$ is formed from k_j-th rows values of matrix X: $x_{k_i j}$ correspond to the j-maximum criterion: $a_{jj} = x_j$ ($i, j = 1, 2, ..., m$; m is the number of criteria), that is the maximum values of all the criteria will appear in the main diagonal of the matrix.

The matrix $P = \|p_{ij}\|$ of the relative losses is made:

$$p_{ij} = \frac{x_j - a_{ij}}{x_j} (p_{ii} = 0; \quad i, j = 1, 2, \ldots, m) \ , \tag{29}$$

Elements p_{ij} of matrix P show how the alternative relatively of the j-th criterion is lost if the i-th criteria is selected as the best one.

Weights $q = (q_1, q_2, \ldots\ q_m)$ can be found from the system:

$$Fq^T = 0, \tag{30}$$

Here, matrix F is as follows:

$$F = \begin{pmatrix} -\sum_{i=1}^{m} p_{i1} & p_{12} & \cdots & p_{1m} \\ p_{21} & -\sum_{i=1}^{m} p_{i2} & & p_{2m} \\ & \cdots & & \\ p_{m1} & p_{m2} & \cdots & -\sum_{i=1}^{m} p_{im} \end{pmatrix}. \tag{31}$$

The method based on the criterion significance loss offsets the drawback of the entropy method. Thus, when the values of a criterion do not considerably differ, the elements p_{ij} of the matrix P of relative loss of criterion impact (Equation (30)) approach zero, while the respective criterion weight increases and has a strong impact on the evaluation. In the case of homogeneity, when the values of one of the criteria are the same in all alternatives, all relative losses of the criterion, as well as its total loss, are equal to zero. Therefore, the linear system of Equation (30) makes no sense because one column of elements in matrix P is equal to zero.

4.5.3. Aggregate Objective Weights—IDOCRIW Method

Using the idea of different significance weights to connect a single overall weight [46,50,63,64], it is possible to connect the entropy weights W_j and weights q_j of the criteria impact loss methods, connecting them to the common objective criteria for the assessment of the structure of the array weights ω_j:

$$\omega_j = \frac{q_j W_j}{\sum_{j=1}^{m} q_j W_j}, \tag{32}$$

These weights will emphasize the separation of the particular values of the criteria (entropy characteristic), but the impact of these criteria is decreased due the higher loss in other criteria.

The calculated weights of the entropy and criteria loss of impact are combined into aggregated weights and then are used in multi-criteria assessment, for ranking of options, and for the selection of the best alternative.

5. Multi-Criteria Analysis of Steel Rope Diagnostics Results

Results of experimental research have a different level of significance. Multi-criteria analysis, in this case, is a tool for optimal solution acceptance in diagnostics. The performed processing of experimental data reveals the power of the applied criteria weight and brings efficiency to the diagnostic procedure. Data for multi-criteria analysis are shown in Table 1.

Evaluation and comparison were performed in the groups of frequencies: f = 60, 110, 160, 210, 260, 310, 360, 410, 460, 510, and 560—in total 11 groups. Each group contains nine alternative cases to be compared. Each case has a different rope length and diameter. For comparison, we use four parameters: vibration amplitudes of the rope surface, and three different lengths of the wire, as presented in Table 1. The criteria weight here is defined using three methods: entropy, CILOS, vand IDOCRIW. The obtained criteria weights were compared by applying four MCDM methods: TOPSIS, COPRAS, EDAS and SAW.

The values of criteria weights are presented in Table A2 (Appendix B). Part of the results are presented graphically in Figures 5 and 6.

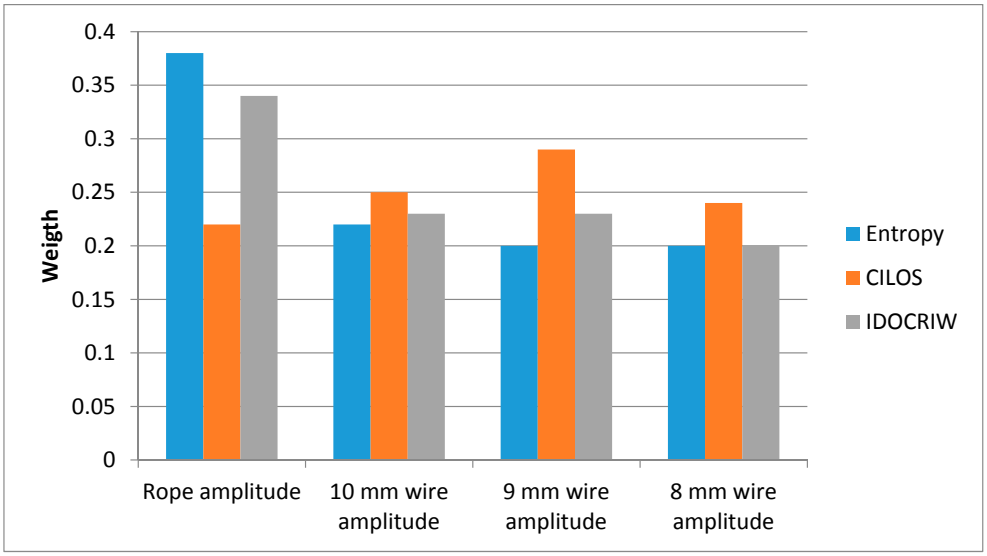

Figure 5. Results of the criteria weight distribution for entropy, Criterion Impact Loss (CILOS) and Integrated Determination of Objective Criteria Weights (IDOCRIW) methods for a 60 Hz vibration frequency.

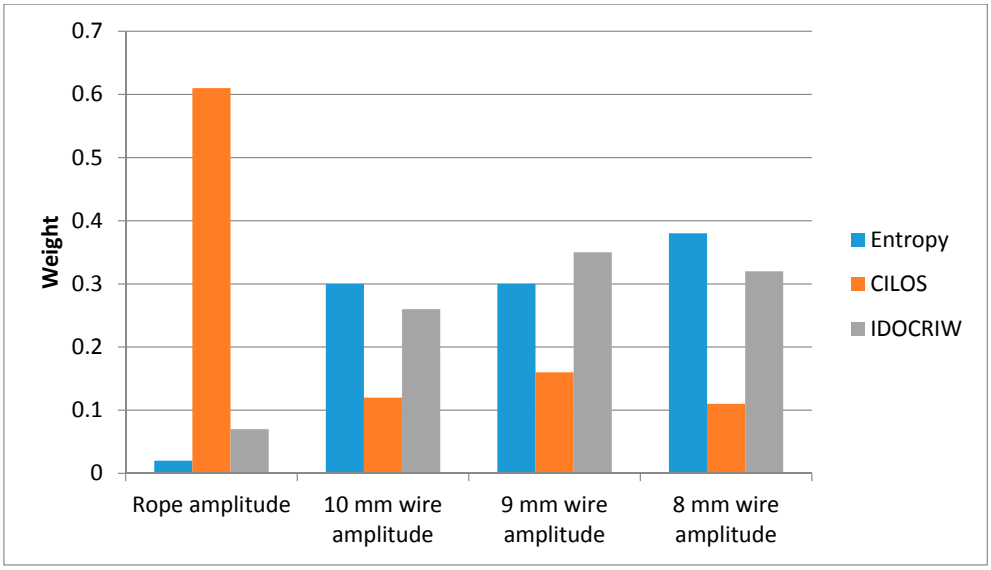

Figure 6. Results of the criteria weight distribution for entropy, CILOS and IDOCRIW methods for a 110 Hz vibration frequency.

Figures 5 and 6 present comparisons of results that are obtained using two methods: entropy and CILOS. Weights of criteria and their difference range using IDOCRIW. Such procedure occurs to

broaden the distribution of results obtained from entropy and CILOS, as shown in Figure 6 for the case of vibration frequency 110 Hz. In this case, generalized weights of IDOCRIW compensate deficiencies of both methods and closer represent structure of the analyzed data. In the case presented in Figure 6, using entropy, Criterion 4 influences evaluation 25 times more than Criterion 1. Implementation of IDOCRIW decreases this difference to 4.6 times. In the practice presented in Figure 5, criteria weight values differ insignificantly. Even in this case, weights obtained using IDOCRIW better represent structure of the data.

A comparison of the efficiency of MCDM is presented in Figures 7 and 8. Every MCDM method has its own peculiarities, therefore, it is most efficient use the mean of all methods. It must be noted that all methods give unified characteristics for the first and last places (in our case, the third and eighth tests).

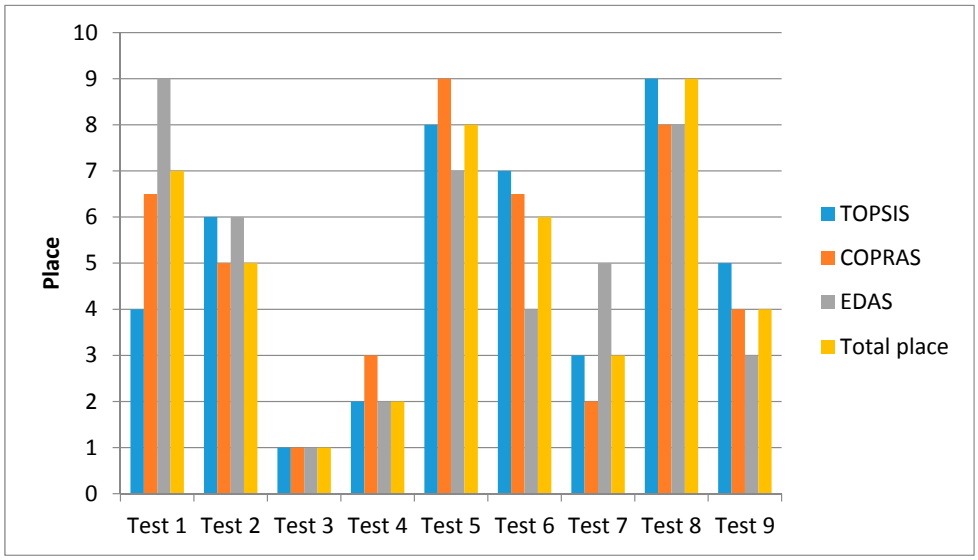

Figure 7. Results of multi-criteria decision-making (MCDM) methods evaluation for The Technique for Order of Preference by Similarity to Ideal Solution (TOPSIS), Complex Proportional Assessment (COPRAS) and Evaluation Based on Distance from Average Solution (EDAS) methods for a 60 Hz vibration frequency.

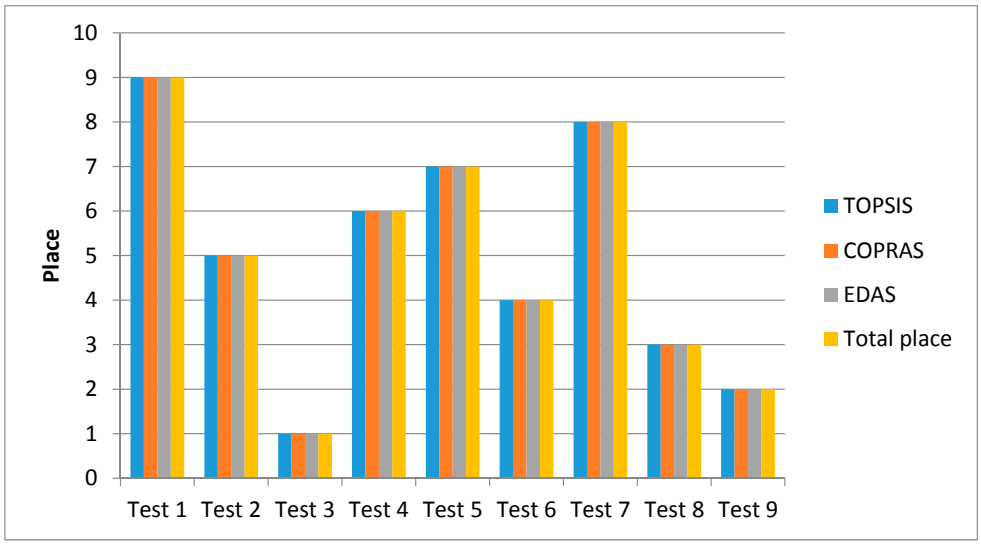

Figure 8. Results of the MCDM evaluation for TOPSIS, COPRAS and EDAS methods for a 110 Hz vibration frequency.

Figures 7 and 8 compare cases of using various MCDM methods. Figure 7 (for the case of 60 Hz) shows a particular case when peculiarities of various MCDM methods cause broad distribution of evaluations and the range used the mean of all method results. Figure 8 (for the case of 110 Hz) presents a very special case of MCDM analysis when all proposed methods are equal in criteria weight. This is very rare in practical cases.

All the results of the MCDM method evaluation are presented in Table A3 (Appendix C).

After processing of the experimental data, significant improvement in the damage criteria can be added. This will increase the diagnostic accuracy and reduce the requirements for measurement equipment. Multi-criteria analysis revealed important issues. According to the analysis shown in Table A3, the most successful are Variants 8 and 9. The analysis of the experimental test results requires additional research on the complexity of physical phenomena-based methods. The sensitivity of the applied MCDM methods differs and EDAS seems to be the most sensitive one. The application of multi-criteria analysis in the field of technical diagnostics seems very promising.

6. Discussion

Human-carrying technical installation with ropes, such as elevators, cable cars, funiculars, and various lifting devices, are widely used nowadays. The increase in the number of these technical installations creates challenges for engineers to create compact, light, and cheap devices, especially in old buildings. Due to the pressure on dimensions, lifting equipment uses small pulleys, which demand the implementation of thin ropes. Thin ropes are more flexible, but more often require a technical inspection, and they are more sensitive to the amount of broken wires per running meter.

Technical diagnostic methods for broken wire detection is a significant issue today, which requires a great amount of time of specialists, while existing equipment hardly finds them due to practical circumstances. The proposed method for broken wire diagnostics is already patented and technically possible, but the analysis of the measurement results requires mathematical procedure for big data processing from extensive diagnostic measurement.

From the data obtained from sensors after signal processing, there are rare cases when the signal reveals a clear case of damage. The detection of damage with high possibility is given by the MCDM methods, which takes into account the general dataset from hardware and derives a solution after an objective data analysis. Subjective evaluation of the criteria weights brings poor results: experts have difficulty in defining the criteria weights. The proposed MCDM analyzes the general dataset and evaluates the structure of the data. Therefore, in technical diagnostics, the implementation of decision-making procedures has great potential.

The widely used method of entropy, which provides criteria value diversification, is not sensitive in the main tasks of diagnostics. Provided by authors, the methods CILOS and generalized criteria weight definition IDOCRIW compensate the short comings of the entropy method.

7. Conclusions

Implementation of MCDM in technical diagnostics opens the possibility of objective parameters analysis without human interference and creates the possibility of implementation in the Internet of Things.

Every MCDM method has its own peculiarities, therefore, it is most efficient to use the means of all methods. The proposed implementation of multi-criteria analysis in technical diagnostics seems promising, but further implementation requires further development of the method. The results of the performed formal analysis of the diagnostic parameters coincide with the most significant diagnostic result, revealed by the extensive expert analysis provided.

Author Contributions: The individual contribution and responsibilities of the authors were as follows: Audrius Čereška provided the idea and extensive advice throughout the study. Vytautas Bucinskas provided the research concept and rope diagnostics methodology. He is the co-author of the diagnostic method and co-inventor of the patent KR20140088149 "Method and equipment of steel rope quality diagnostics".

Edmundas Kazimieras Zavadskas provided and designed the research concept for MCDM implementation in the diagnostic area. He is the co-author of the methods COPRAS, EDAS, CILOS and IDOCRIW. Valentinas Podvezko collected and analyzed the data. He is the co-author of the methods CILOS, and IDOCRIW, and the author of software for the implementation of the method. Ernestas Sutinys performed the experimental research, provided the experimental data, and revised the manuscript. He is the co-inventor of the method and patent KR20140088149 "Method and equipment of steel rope quality diagnostics". All authors have read and approved the final manuscript.

Conflicts of Interest: The authors declare no conflict of interest.

Appendix A

Table A1. Rope vibration experimental data.

Item No.	Frequency, Hz	Rope Length, mm	Rope Diameter, mm	Rope Amplitude, mm	10 mm Wire Amplitude, mm	9 mm Wire Amplitude, mm	8 mm Wire Amplitude, mm
1	60	1350	3.92	0.082	0.237	0.223	0.233
2		1450		0.124	0.226	0.362	0.295
3		1550		0.119	0.364	0.385	0.402
4		1350	3.96	0.087	0.284	0.291	0.289
5		1450		0.110	0.228	0.279	0.299
6		1550		0.120	0.288	0.285	0.287
7		1350	4.0	0.056	0.199	0.231	0.212
8		1450		0.132	0.305	0.294	0.291
9		1550		0.121	0.299	0.288	0.301
1	110	1350	3.92	3.648	0.198	0.184	0.174
2		1450		3.502	0.202	0.226	0.235
3		1550		3.495	0.351	0.352	0.349
4		1350	3.96	3.523	0.214	0.199	0.174
5		1450		3.891	0.198	0.199	0.188
6		1550		3.315	0.258	0.281	0.252
7		1350	4.0	3.598	0.184	0.201	0.187
8		1450		3.871	0.279	0.284	0.289
9		1550		3.498	0.288	0.283	0.286
1	160	1350	3.92	3.384	11.600	10.100	11.400
2		1450		3.498	11.625	12.304	10.800
3		1550		3.436	10.998	11.462	9.511
4		1350	3.96	3.510	10.989	11.056	11.104
5		1450		3.820	12.056	12.002	11.992
6		1550		3.297	11.997	12.102	12.099
7		1350	4.0	3.502	12.078	12.106	12.098
8		1450		3.862	12.135	12.104	12.145
9		1550		3.411	12.141	12.097	12.112
1	210	1350	3.92	3.421	0.472	0.431	0.498
2		1450		3.514	0.497	0.453	0.496
3		1550		3.458	0.652	0.681	0.521
4		1350	3.96	3.519	0.512	0.618	0.561
5		1450		3.87	0.741	0.739	0.731
6		1550		3.341	0.769	0.763	0.778
7		1350	4.0	3.541	0.674	0.614	0.689
8		1450		3.878	0.781	0.798	0.756
9		1550		3.489	0.821	0.851	0.849
1	260	1350	3.92	0.631	0.571	0.594	0.621
2		1450		0.645	0.624	0.681	0.570
3		1550		0.687	0.734	0.690	0.543
4		1350	3.96	0.636	0.732	0.741	0.735
5		1450		0.634	0.764	0.744	0.752
6		1550		0.702	0.778	0.802	0.803
7		1350	4.0	0.628	0.812	0.807	0.799
8		1450		0.644	0.823	0.851	0.853
9		1550		0.732	0.824	0.856	0.854
1	310	1350	3.92	1.352	0.045	0.034	0.051
2		1450		0.702	0.057	0.059	0.051
3		1550		0.706	0.055	0.061	0.054
4		1350	3.96	0.581	0.053	0.047	0.051
5		1450		0.756	0.058	0.061	0.059
6		1550		0.754	0.056	0.055	0.053
7		1350	4.0	0.768	0.058	0.059	0.057
8		1450		0.708	0.052	0.059	0.051
9		1550		0.812	0.067	0.061	0.066

Table A1. *Cont.*

Item No.	Frequency, Hz	Rope Length, mm	Rope Diameter, mm	Rope Amplitude, mm	10 mm Wire Amplitude, mm	9 mm Wire Amplitude, mm	8 mm Wire Amplitude, mm
1	360	1350	3.92	0.421	0.063	0.066	0.064
2		1450		0.523	0.061	0.062	0.071
3		1550		0.498	0.059	0.064	0.074
4		1350	3.96	0.396	0.071	0.068	0.069
5		1450		0.499	0.070	0.076	0.071
6		1550		0.501	0.069	0.071	0.074
7		1350	4.0	0.562	0.068	0.069	0.065
8		1450		0.485	0.071	0.068	0.063
9		1550		0.456	0.069	0.066	0.070
1	410	1350	3.92	1.638	0.052	0.049	0.047
2		1450		1.625	0.049	0.045	0.043
3		1550		1.603	0.051	0.059	0.061
4		1350	3.96	1.624	0.049	0.061	0.058
5		1450		1.53	0.064	0.074	0.069
6		1550		1.561	0.062	0.063	0.061
7		1350	4.0	1.821	0.061	0.062	0.059
8		1450		1.509	0.064	0.067	0.061
9		1550		1.598	0.062	0.061	0.065
1	460	1350	3.92	1.399	0.172	0.160	0.088
2		1450		1.502	0.163	0.149	0.162
3		1550		1.526	0.161	0.164	0.142
4		1350	3.96	1.480	0.168	0.174	0.175
5		1450		1.499	0.170	0.181	0.173
6		1550		1.541	0.179	0.178	0.172
7		1350	4.0	1.474	0.186	0.192	0.191
8		1450		1.501	0.198	0.191	0.192
9		1550		1.556	0.201	0.187	0.206
1	510	1350	3.92	1.483	0.187	0.198	0.079
2		1450		1.586	0.151	0.148	0.154
3		1550		1.617	0.158	0.159	0.139
4		1350	3.96	1.571	0.147	0.134	0.151
5		1450		1.521	0.164	0.163	0.165
6		1550		1.601	0.169	0.164	0.171
7		1350	4.0	1.541	0.145	0.141	0.144
8		1450		1.515	0.181	0.19	0.184
9		1550		1.571	0.181	0.179	0.175
1	560	1350	3.92	1.177	0.284	0.236	0.201
2		1450		1.402	0.301	0.218	0.321
3		1550		1.322	0.371	0.382	0.375
4		1350	3.96	1.180	0.381	0.395	0.386
5		1450		1.351	0.406	0.398	0.391
6		1550		1.298	0.401	0.405	0.415
7		1350	4.0	1.157	0.501	0.498	0.475
8		1450		1.243	0.503	0.525	0.504
9		1550		1.324	0.499	0.520	0.521

Appendix B

Table A2. Comparison between MCDM methods of entropy, CILOS and IDOCRIW.

Frequency Hz	Weight Definition Method	Rope Amplitude, mm	10 mm Wire Amplitude, mm	9 mm Wire Amplitude, mm	8 mm Wire Amplitude, mm
60	Entropy	0.3821	0.2228	0.1968	0.1984
	CILOS	0.217	0.253	0.287	0.243
	IDOCRIW	0.340	0.231	0.231	0.198
110	Entropy	0.0154	0.2985	0.3013	0.3840
	CILOS	0.612	0.119	0.156	0.113
	IDOCRIW	0.0696	0.2629	0.3470	0.3204
160	Entropy	0.1996	0.1092	0.2651	0.4261
	CILOS	0.053	0.218	0.581	0.148
	IDOCRIW	0.0421	0.0947	0.6125	0.2508
210	Entropy	0.0197	0.3037	0.3677	0.3089
	CILOS	0.387	0.259	0.159	0.196
	IDOCRIW	0.0372	0.3831	0.2848	0.2949
260	Entropy	0.0535	0.2522	0.2280	0.4663
	CILOS	0.065	0.632	0.161	0.143
	IDOCRIW	0.0131	0.5986	0.1379	0.2505

Table A2. *Cont.*

Frequency Hz	Weight Definition Method	Rope Amplitude, mm	10 mm Wire Amplitude, mm	9 mm Wire Amplitude, mm	8 mm Wire Amplitude, mm
310	Entropy	0.5726	0.0959	0.2588	0.0726
	CILOS	0.231	0.170	0.438	0.161
	IDOCRIW	0.4834	0.0596	0.4143	0.0427
360	Entropy	0.4876	0.2031	0.1548	0.1546
	CILOS	0.115	0.258	0.129	0.498
	IDOCRIW	0.2730	0.2551	0.0972	0.3748
410	Entropy	0.0516	0.2310	0.3638	0.3536
	IDOCRIW	0.0516	0.2310	0.3638	0.3536
460	Entropy	0.015	0.104	0.114	0.767
	CILOS	0.463	0.239	0.216	0.081
	IDOCRIW	0.0575	0.2108	0.2073	0.5243
510	Entropy	0.0108	0.1222	0.2338	0.6332
	CILOS	0.451	0.297	0.236	0.017
	IDOCRIW	0.0454	0.3388	0.5153	0.1005
560	Entropy	0.0236	0.2138	0.4272	0.3354
	CILOS	0.071	0.691	0.135	0.102
	IDOCRIW	0.0069	0.6122	0.2390	0.1418

Appendix C

Table A3. Results of MCDM methods evaluation.

Frequency Hz	Cases	1	2	3	4	5	6	7	8	9
	Methods									
60	TOPSIS	0.426	0.332	0.538	0.524	0.309	0.315	0.516	0.308	0.339
	Place	4	6	1	2	8	7	3	9	5
	COPRAS-SAW	0.105	0.105	0.130	0.117	0.102	0.105	0.121	0.105	0.107
	Place	6-7	5	1	3	9	6-7	2	8	4
	EDAS	0.290	0.330	0.868	0.650	0.326	0.367	0.348	0.309	0.407
	Place	9	6	1	2	7	4	5	8	3
	Sum of the places	19.5	17	3	7	24	17.5	10	25	12
	Total places	7	5	1	2	8	6	3	9	4
110	TOPSIS	0.041	0.265	0.990	0.101	0.084	0.496	0.078	0.611	0.616
	Place	9	5	1	6	7	4	8	3	2
	COPRAS-SAW	0.086	0.103	0.158	0.091	0.090	0.121	0.089	0.128	0.130
	Place	9	5	1	6	7	4	8	3	2
	EDAS	0.0	0.336	1	0.092	0.080	0.611	0.062	0.684	0.703
	Place	9	5	1	6	7	4	8	3	2
	Sum of the places	27	15	3	18	21	12	24	9	6
	Total places	9	5	1	6	7	4	8	3	2
160	TOPSIS	0.264	0.799	0.494	0.466	0.867	0.917	0.717	0.905	0.916
	Place	9	6	7	8	5	1	2	4	3
	COPRAS-SAW	0.101	0.112	0.104	0.105	0.114	0.115	0.115	0.115	0.115
	Place	9	6	8	7	5	1-2	3	4	1-2
	EDAS	0.021	0.813	0.158	0.225	0.855	1.0	0.979	0.970	0.998
	Place	9	6	8	7	5	1	3	4	2
	Sum of the places	27	18	23	22	15	3.5	8	12	6,5
	Total places	9	6	8	7	5	1	3	4	2
210	TOPSIS	0.015	0.055	0.439	0.267	0.729	0.816	0.523	0.833	0.995
	Place	9	8	6	7	4	3	5	2	1
	COPRAS-SAW	0.080	0.082	0.105	0.095	0.123	0.129	0.111	0.130	0.140
	Place	9	8	6	7	4	3	5	2	1
	EDAS	0.003	0.043	0.404	0.239	0.715	0.815	0.512	0.827	1.0
	Place	9	8	6	7	4	3	5	2	1
	Sum of the places	27	24	18	21	12	9	15	6	3
	Total Places	9	8	6	7	4	3	5	2	1
260	TOPSIS	0.106	0.196	0.500	0.629	0.733	0.820	0.904	0.994	0.991
	Place	9	8	7	6	5	4	3	1	2
	COPRAS-SAW	0.088	0.093	0.102	0.110	0.114	0.118	0.121	0.125	0.125
	Place	9	8	7	6	5	4	3	1-2	1-2
	EDAS	0.002	0.102	0.302	0.493	0.606	0.751	0.859	0.993	0.997
	Place	9	8	7	6	5	4	3	2	1
	Sum of the places	27	24	21	18	15	12	9	4.5	4.5
	Total Places	9	8	7	6	5	4	3	1-2	1-2

Table A3. *Cont.*

Frequency Hz	Cases	1	2	3	4	5	6	7	8	9
310	TOPSIS	0.0	0.852	0.851	0.814	0.796	0.774	0.777	0.842	0.734
	Place	9	1	2	4	5	7	6	3	8
	COPRAS-SAW	0.068	0.118	0.119	0.119	0.116	0.111	0.114	0.117	0.114
	Place	9	3	2	1	5	8	7	4	6
	EDAS	0.0	0.830	0.875	0.935	0.781	0.592	0.689	0.807	0.740
	Place	9	3	2	1	5	8	7	4	6
	Sum of the places	27	7	6	6	15	23	20	11	20
	Total Places	9	3	1-2	1-2	5	8	6-7	4	6-7
360	TOPSIS	0.554	0.366	0.480	0.788	0.546	0.570	0.259	0.446	0.650
	Place	4	8	6	1	5	3	9	7	2
	COPRAS-SAW	0.110	0.106	0.109	0.119	0.113	0.114	0.104	0.108	0.113
	Place	5	8	6	1	4	2	9	7	3
	EDAS	0.454	0.186	0.379	1.0	0.683	0.713	0.047	0.375	0.699
	Place	5	8	6	1	4	2	9	7	3
	Sum of the places	14	24	18	3	13	7	27	21	8
	Total Places	5	8	6	1	4	2	9	7	3
410	TOPSIS	0.150	0.025	0.545	0.526	0.997	0.663	0.609	0.739	0.676
	Place	8	9	6	7	1	4	5	2	3
	COPRAS-SAW	0.093	0.087	0.109	0.107	0.131	0.117	0.114	0.121	0.118
	Place	8	9	6	7	1	4	5	2	3
	Sum of the places	16	18	12	14	2	8	10	4	3
	Total Places	8	9	6	7	1	4	5	2	3
460	TOPSIS	0.050	0.600	0.448	0.719	0.708	0.705	0.866	0.882	0.977
	Place	9	7	8	4	5	6	3	2	1
	COPRAS-SAW	0.081	0.104	0.098	0.112	0.113	0.113	0.123	0.124	0.129
	Place	9	7	8	6	5	4	3	2	1
	EDAS	0.011	0.384	0.295	0.557	0.564	0.562	0.824	0.870	0.996
	Place	9	7	8	6	4	5	3	2	1
	Sum of the places	27	21	24	16	14	15	9	6	3
	Total Places	9	7	8	6	4	5	3	2	1
510	TOPSIS	0.760	0.277	0.397	0.178	0.486	0.519	0.193	0.878	0.736
	Place	2	7	6	9	5	4	8	1	3
	COPRAS-SAW	0.123	0.102	0.106	0.096	0.111	0.113	0.098	0.126	0.121
	Place	2	7	6	9	5	4	8	1	3
	EDAS	0.820	0.203	0.350	0.0	0.514	0.565	0.054	0.945	0.809
	Place	2	7	6	9	5	4	8	1	3
	Sum of the places	6	21	18	27	15	12	24	3	9
	Total Places	2	7	6	9	5	4	8	1	3
560	TOPSIS	0.026	0.120	0.439	0.482	0.566	0.560	0.943	0.984	0.982
	Place	9	8	7	6	4	5	3	1	2
	COPRAS-SAW	0.072	0.078	0.003	0.106	0.110	0.111	0.137	0.140	0.139
	Place	9	8	7	6	5	4	3	1	2
	EDAS	0.001	0.081	0.401	0.440	0.498	0.510	0.944	1.0	0.994
	Place	9	8	7	6	5	4	3	1	2
	Sum of the places	27	24	21	18	14	13	9	3	6
	Total Places	9	8	7	6	5	4	3	1	2

References

1. Bucinskas, V.; Sutinys, E.; Augustaitis, V.K. Experimental research of steel rope integrity problem. *J. Vibroeng.* **2011**, *13*, 312–318.
2. Basak, D.; Pal, S.; Patranabis, D.C. Inspection 6X19 Seale Preformed Haulage Rope by Nondestructive Technique. *Russ. J. Nondestruct. Test.* **2009**, *45*, 143–147. [CrossRef]
3. Basak, D.; Pal, S.; Patranabis, D.C. Non-destructive Evaluation of a 6X25 FW Haulage Rope in a Monocable Continuously Moving Passenger Cable Car Installation. *Int. J. Eng. Technol.* **2009**, *5*, 486–490. [CrossRef]
4. Sutinys, E.; Bucinskas, V. Detecting defects rope using dynamical methods. In Proceedings of the 16th International Conference, Kaunas, Lithuania, 7–8 April 2011; Kaunas University of Technology: Kaunas, Lithuania, 2011.
5. Sutinys, E.; Bucinskas, V.; Dzedzickis, A. The Research of Wire Rope Defect Using Contactless Dynamic Method. *Solid State Phenom.* **2016**, *251*, 49–54. [CrossRef]

6. Peterka, P.; Kresak, J.; Kropuch, S.; Fedorko, G.; Molnar, V.; Vojtko, M. Failure Analysis of Hoisting Steel Wire Rope. *Eng. Fail. Anal.* **2014**, *45*, 96–105. [CrossRef]
7. Vukelic, G.; Vizentin, G. Damage-induced stresses and remaining service life predictions of wire ropes. *Appl. Sci.* **2017**, *7*, 107. [CrossRef]
8. Zhang, Y.; Li, D.; Zhou, Z. Time reversal method for guided waves with multimode and multipath on corrosion defect detection in wire. *Appl. Sci.* **2017**, *7*, 424. [CrossRef]
9. Liu, Z.; Guo, T.; Chai, S. Probabilistic fatigue life prediction of bridge cables based on multiskilling and mesoscopic fracture mechanics. *Appl. Sci.* **2016**, *6*, 99. [CrossRef]
10. Khan, F.; Bartoli, I.; Vanniamparambil, P.A.; Carmi, R.; Rajaram, S.; Kontsos, A. Integrated health monitoring system for damage detection in civil structural components. In *Safety, Reliability, Risk and Life-Cycle Performance of Structures and Infrastructures, Proceedings of the 11th International Conference on Structural Safety and Reliability, New York, NY, USA, 16–20 June 2013*; Deodatis, G., Ellingwood, B.R., Frangopol, D.M., Eds.; Taylor & Francis Group: London, UK, 2013.
11. Fedorko, G.; Molnar, V.; Ferková, Ž.; Peterka, P.; Krešák, J.; Tomašková, M. Possibilities of failure analysis for steel cord conveyor belts using knowledge obtained from non-destructive testing of steel ropes. *Eng. Fail. Anal.* **2016**, *67*, 33–45. [CrossRef]
12. Zhang, J.; Tan, X.; Zheng, P. Non-destructive detection of wire rope discontinuities from residual magnetic field images using the hilbert-huang transform and compressed sensing. *Sensors* **2017**, *17*, 608. [CrossRef] [PubMed]
13. Qiao, T.Z.; Li, Z.X.; Jin, B.Q. Identification of mining steel rope broken wires based on improved EEMD. *Int. J. Min. Miner. Eng.* **2016**, *7*, 224–236. [CrossRef]
14. Giglio, M.; Manes, A. A Life Prediction of a Wire Rope Subjected to Axial and Bending Loads. *Eng. Fail. Anal.* **2005**, *12*, 549–568. [CrossRef]
15. Elata, D.; Eshkenazy, R.; Weiss, M.P. The Mechanical Behavior of a Wire Rope with an Independent Wire Rope Core. *Int. J. Solids Struct.* **2004**, *41*, 1157–1172. [CrossRef]
16. Zhang, D.K.; Ge, S.R.; Qiang, Y.H. Research on the Fatigue and Fracture Behavior Due to the Fretting Wear of Steel Wire in Hoisting Rope. *Wear* **2003**, *255*, 1233–1237. [CrossRef]
17. Paczelt, I.; Beleznai, R. Nonlinear Contact—Theory for Analysis of Wire Rope Strand Approximation in the FEM. *J. Comput. Struct.* **2011**, *89*, 1004–1025. [CrossRef]
18. Ghoreishi, S.R.; Cartroud, P.; Davies, P.; Messager, T. Analytical Modelling of Synthetic Fiber Ropes Subjected to Axial Loads. Part I: A continuum model for multilayered fibrous structures. *Int. J. Solids Struct.* **2007**, *44*, 2924–2942. [CrossRef]
19. Ghoreishi, S.R.; Cartroud, P.; Davies, P.; Messager, T. Analytical Modelling of Synthetic Fiber Ropes Subjected to Axial Loads. Part II: A linear elastic model for 1+6 fibrous structures. *Int. J. Solids Struct.* **2007**, *44*, 2943–2960. [CrossRef]
20. Shibu, G.; Mohankumar, K.V.; Devendiran, S. Analysis of a Three Layered Straight Wire Rope Strand Using Finite Element Method. Lecture Notes in Engineering and Computer. In Proceedings of the Word Congress on Engineering, London, UK, 6–9 July 2011.
21. Wang, X.Y.; Meng, X.B.; Wang, J.X.; Sun, Y.H.; Gao, K. Mathematical Modeling and Geometric Analysis for Wire Rope Strands. *Appl. Math. Model.* **2015**, *39*, 1019–1032. [CrossRef]
22. Raisutis, R.; Kazys, L.; Mažeika, L.; Zukauskas, E.; Samaitis, V.; Jankauskas, A. Ultrasonic Guided Wave-Based Testing Technique for Inspection of Multi-Wire Rope Structures. *NDT E Int.* **2014**, *62*, 40–49. [CrossRef]
23. Zhang, D.; Zhao, M.; Zhou, Z.; Pan, S. Characterization of Wire Rope Defects with Gray Level Co-occurrence Matrix of Magnetic Flux Leakage Images. *J. Nondestruct. Eval.* **2013**, *32*, 37–43. [CrossRef]
24. Wang, Y.; Liu, X.; Wu, B.; Xiao, J.; Wu, D.; He, C. Dipole modeling of stress-dependent magnetic flux leakage. *NDT E Int.* **2018**, *95*, 1–8. [CrossRef]
25. Wu, B.; Wang, Y.J.; Liu, X.C.; He, C.F. A novel TMR-based MFL sensor for steel wire rope inspection using the orthogonal test method. *Smart Mater. Struct.* **2015**, *24*, 1–12. [CrossRef]
26. Rashidi, M.; Ghodrat, M.; Samali, B.; Kendall, B.; Zhang, C.W. Remedial Modelling of Steel Bridges through Application of Analytical Hierarchy Process (AHP). *Appl. Sci.* **2017**, *7*, 168. [CrossRef]
27. Terracciano, G.; Di Lorenzo, G.; Formisano, A.; Landolfo, R. Cold-formed thin-walled steel structures as vertical addition and energetic retrofitting systems of existing masonry buildings. *Eur. J. Environ. Civil Eng.* **2015**, *19*, 850–866. [CrossRef]

28. Shahriar, A.; Modirzadeh, M.; Sadiq, R.; Tesfamariam, S. Seismic induced damageability evaluation of steel buildings: A Fuzzy-TOPSIS method. *Earthq. Struct.* **2012**, *3*, 695–717. [CrossRef]
29. Sanchez-Lozano, J.M.; Meseguer-Valdenebro, J.L.; Portoles, A. Assessment of Arc Welding Process through the Combination of TOPSIS-AHP Methods with Fuzzy Logic. *Trans. Indian Inst. Met.* **2017**, *70*, 935–946. [CrossRef]
30. Madic, M.; Antucheviciene, J.; Radovanovic, M.; Petkovic, D. Determination of laser cutting process conditions using the preference selection index method. *Opt. Laser Technol.* **2017**, *89*, 214–220. [CrossRef]
31. Yin, H.F.; Xiao, Y.Y.; Wen, G.L.; Qing, Q.X.; Deng, Y.F. Multiobjective optimization for foam-filled multi-cell thin-walled structures under lateral impact. *Thin-Walled Struct.* **2015**, *94*, 1–12. [CrossRef]
32. Fang, J.G.; Gao, Y.K.; Sun, G.Y.; Qiu, N.; Li, Q. On design of multi-cell tubes under axial and oblique impact loads. *Thin-Walled Struct.* **2015**, *95*, 115–126. [CrossRef]
33. Rezvani, M.J.; Jahan, A. Effect of initiator, design, and material on crashworthiness performance of thin-walled cylindrical tubes: A primary multi-criteria analysis in lightweight design. *Thin-Walled Struct.* **2015**, *96*, 169–182. [CrossRef]
34. Pirmohammad, S.; Marzdashti, S.E. Crushing behavior of new designed multi-cell members subjected to axial and oblique quasi-static loads. *Thin-Walled Struct.* **2016**, *108*, 291–304. [CrossRef]
35. Zheng, G.; Wu, S.Z.; Sun, G.Y.; Li, G.Y.; Li, Q. Crushing analysis of foam-filled single and bitubal polygonal thin-walled tubes. *Int. J. Mech. Sci.* **2014**, *87*, 226–240. [CrossRef]
36. Qiu, N.; Gao, Y.K.; Fang, J.G.; Feng, Z.X.; Sun, G.Y.; Li, Q. Crashworthiness analysis and design of multi-cell hexagonal columns under multiple loading cases. *Finite Elements Anal. Des.* **2015**, *104*, 89–101. [CrossRef]
37. Esmaeili-Marzdashti, S.; Pirmohammad, S. Crashworthiness Analysis of S-Shaped Structures Under Axial Impact Loading. *Lat. Am. J. Solids Struct.* **2017**, *14*, 743–764. [CrossRef]
38. Bitarafan, M.; Hashemkhani Zolfani, S.; Arefi, S.L.; Zavadskas, E.K. Evaluating the construction methods of cold-formed steel structures in reconstructing the areas damaged in natural crises, using the methods AHP and COPRAS-G. *Arch. Civil Mech. Eng.* **2012**, *12*, 360–367. [CrossRef]
39. Maity, S.R.; Chatterjee, P.; Chakraborty, S. Cutting tool material selection using grey complex proportional assessment method. *Mater. Des.* **2012**, *36*, 372–378. [CrossRef]
40. Chatterjee, P.; Athawale, V.M.; Chakraborty, S. Materials selection using complex proportional assessment and evaluation of mixed data methods. *Mater. Des.* **2011**, *32*, 851–860. [CrossRef]
41. Chatterjee, P.; Chakraborty, S. Material selection using preferential ranking methods. *Mater. Des.* **2012**, *35*, 384–393. [CrossRef]
42. Mousavi-Nasab, S.H.; Sotoudeh-Anvari, A. A comprehensive MCDM-based approach using TOPSIS, COPRAS and DEA as an auxiliary tool for material selection problems. *Mater. Des.* **2017**, *121*, 237–253. [CrossRef]
43. Yazdani, M.; Jahan, A.; Zavadskas, E.K. Analysis in material selection: Influence of normalization tools on COPRAS-G. *Econ. Comput. Econ. Cybern. Stud. Res.* **2017**, *51*, 59–74.
44. Nguyen, H.T.; Dawal, S.Z.M.; Nukman, Y.; Aoyama, H.; Case, K. An Integrated Approach of Fuzzy Linguistic Preference Based AHP and Fuzzy COPRAS for Machine Tool Evaluation. *PLoS ONE* **2015**, *10*, 24. [CrossRef] [PubMed]
45. Keshavarz Ghorabaee, M.; Zavadskas, E.K.; Olfat, L.; Turskis, Z. Multi-Criteria Inventory Classification Using a New Method of Evaluation Based on Distance from Average Solution (EDAS). *Informatica* **2015**, *26*, 435–451. [CrossRef]
46. Hwang, C.L.; Yoon, K. *Multiple Attribute Decision Making Methods and Applications: A State of the Art Survey*; Springer–Verlag: Berlin, Germany, 1981.
47. Zavadskas, E.K.; Kaklauskas, A.; Šarka, V. The new method of multi-criteria complex proportional assessment of projects. *Technol. Econ. Dev. Econ.* **1994**, *1*, 131–139.
48. Shannon, C.E. A mathematical theory of communication. *Bell Syst. Tech. J.* **1948**, *27*, 623–656. [CrossRef]
49. Mirkin, B.G. *Group Choice*; Winston&Sons: Wachington, DC, USA, 1979.
50. Zavadskas, E.K.; Podvezko, V. Integrated determination of objective criteria weights in MCDM. *Int. J. Inf. Technol. Decis. Mak.* **2016**, *15*, 267–283. [CrossRef]
51. Xiang, L.; Wang, H.Y.; Chen, Y.; Guan, Y.J.; Wang, Y.L.; Dai, L.H. Modeling of multi-strand wire ropes subjected to axial tension and torsion loads. *Int. J. Solids Struct.* **2015**, *58*, 233–246. [CrossRef]

52. Monsivais, G.; Diaz-de-Anda, A.; Flores, J.; Gutierrez, L.; Morales, A. Experimental study of the Timoshenko beam theory predictions: Further results. *J. Sound Vib.* **2016**, *375*, 187–199. [CrossRef]
53. Franco-Villafane, J.A.; Mendez-Sanchez, R.A. On the accuracy of the Timoshenko beam theory above the critical frequency: Best shear coefficient. *J. Mech.* **2016**, *32*, 515–518. [CrossRef]
54. Gul, U.; Aydogdu, M. Wave Propagation Analysis in Beams Using Shear Deformable Beam Theories Considering Second Spectrum. *J. Mech.* **2017**, 1–11. [CrossRef]
55. Mardani, A.; Jusoh, A.; MD Nor, K.; Khalifah, Z.; Zakwan, N.; Valipour, A. Multiple criteria decision-making techniques and their applications—A review of the literature from 2000 to 2014. *Econ. Res. Ekon. Istraž.* **2015**, *28*, 516–571. [CrossRef]
56. Zavadskas, E.K.; Mardani, A.; Turskis, Z.; Jusoh, A.; Nor, K.M.D. Development of TOPSIS method to solve complicated decision-making problems: An overview on developments from 2000 to 2015. *Int. J. Inf. Technol. Decis. Mak.* **2016**, *15*, 645–682. [CrossRef]
57. Stefano, N.M.; Casarotto Filho, N.; Vergara, L.G.L.; Rocha, R.U.G. COPRAS (complex proportional assessment): State of the art research and its applications. *IEEE Lat. Am. Trans.* **2015**, *13*, 3899–3906. [CrossRef]
58. Čereška, A.; Podvezko, V.; Zavadskas, E.K. Operating characteristics analysis of rotor systems using MCDM methods. *Stud. Inf. Control* **2016**, *25*, 59–68. [CrossRef]
59. Čereška, A.; Zavadskas, E.K.; Cavallaro, F.; Podvezko, V.; Tetsman, I.; Grinbergiene, I. Sustainable assessment of aerosol pollution decrease applying multiple attribute decision-making methods. *Sustainability* **2016**, *8*, 586. [CrossRef]
60. Trinkuniene, E.; Podvezko, V.; Zavadskas, E.K.; Joksiene, I.; Vinogradova, I.; Trinkunas, V. Evaluation of quality assurance in contractor contracts by multi-attribute decision-making methods. *Econ. Res. Ekon. Istraz.* **2017**, *30*, 1152–1180. [CrossRef]
61. Zavadskas, E.K.; Cavallaro, F.; Podvezco, V.; Ubarte, I.; Kaklauskas, A. MCDM assessment of a healthy and safe built environment according to sustainable development principles: A practical neighbourhood approach in Vilnius. *Sustainability* **2017**, *9*, 702. [CrossRef]
62. Han, J.; Li, Y.; Kang, J.; Cai, E.; Tong, Z.; Ouyang, G.; Li, X. Global synchronization of multichannel EEG based on rényi entropy in children with autism spectrum disorder. *Appl. Sci.* **2017**, *7*, 257. [CrossRef]
63. Ma, J.; Fan, Z.P.; Huang, L.H. A subjective and objective integrated approach to determine attribute weights. *Eur. J. Oper. Res.* **1999**, *112*, 397–404. [CrossRef]
64. Lazauskaite, D.; Burinskiene, M.; Podvezko, V. Subjectively and objectively integrated assessment of the quality indices of the suburban residential environment. *Int. J. Strateg. Prop. Manag.* **2015**, *19*, 297–308. [CrossRef]